

Nonlinear Electromagnetic X Waves

C. Conti,¹ S. Trillo,^{1,2} P. Di Trapani,³ G. Valiulis,⁴ A. Piskarskas,⁴ O. Jedrkiewicz,³ and J. Trull^{3,*}

¹*Istituto Nazionale di Fisica della Materia (INFN)-RM3, Via della Vasca Navale 84, 00146 Roma, Italy*

²*Department of Engineering, University of Ferrara, Via Saragat 1, 44100 Ferrara, Italy*

³*INFN and Department of Chemical, Physical and Mathematical Sciences, University of Insubria, Via Valleggio 11, 22100 Como, Italy*

⁴*Department of Quantum Electronics, Vilnius University, Sauletekio Avenue 9, LT-2040 Vilnius, Lithuania*

(Received 23 April 2002; published 2 May 2003)

Nonlinear optical media that are normally dispersive support a new type of localized (nondiffractive and nondispersive) wave packets that are X shaped in space and time and have slower than exponential decay. High-intensity X waves, unlike linear ones, can be formed spontaneously through a trigger mechanism of conical emission, thus playing an important role in experiments.

DOI: 10.1103/PhysRevLett.90.170406

PACS numbers: 03.50.De, 05.45.Yv, 42.65.Jx, 42.65.Tg

The nonlinear response of condensed matter can compensate for the diffractive spreading of optical beams, or the dispersive broadening of pulses due to group-velocity dispersion (GVD), forming spatial [1] or temporal solitons [2], respectively. Recent experimental results concerning the self-focusing behavior of intense ultrashort pulses [3–8] indicate, however, that the spatial and temporal degrees of freedom cannot be treated separately. When the three length scales naturally associated with diffraction, GVD, and nonlinearity become comparable, the most intriguing consequence of space-time coupling is the possibility to form a nondiffractive and nondispersive localized wave packet (LWP), namely, a spatiotemporal soliton or light bullet [9] characterized by *exponentially* decaying tails. A strict constraint for the formation of light bullets is that the nonlinear phase changes counteract both the linear wave-front curvature and the GVD-induced chirp, leading to space-time focusing, as occurring in Kerr-like focusing media with anomalous GVD [5,6].

Vice versa, a normal GVD rules out the possibility to achieve bullet-type LWPs, rather inducing qualitatively different behaviors such as temporal splitting and spectral breaking [3–5,10]. This is the reason why no attempts have been made to answer the fundamental question as to *whether any form of nonlinearity-induced localization could still take place in normally dispersive media*. In this Letter, we show that LWPs do exist also with normal GVD in the form of *nonlinear X waves* (NLXWs) or X-wave solitons. To date X-shaped waves are known only in the context of *linear* acoustic [11] or electromagnetic [12] propagation, and constitute the polichromatic generalization of diffraction-free Bessel (or Durnin [13]) beams. They have been observed in both acoustical [14] and optical [15] experiments, both requiring input beam-shaping techniques. Here we find propagation-invariant NLXWs that can be naturally regarded as the continuation of linear X waves into the nonlinear regime. Yet we find a *fundamental difference* between the linear and nonlinear regimes. NLXWs can be generated sponta-

neously at high intensity from conventional bell-shaped (in space and time) input beams through self-induced spectral reshaping triggered by conical emission.

To be more general we analyze two different phenomena: self-action of a scalar envelope wave packet u_1 (carrier ω_0) due to a pure (cubic) focusing Kerr effect [3–5] or generation of a u_2 envelope at second-harmonic (SH, $2\omega_0$) in noncentrosymmetric (quadratic) media [6]. In the paraxial regime, the evolution in Kerr media is ruled by the scalar 1 + 3 nonlinear Schrödinger (NLS) equation,

$$i\partial_\zeta u_1 + \nabla_\perp^2 u_1 - d_1 \partial_{\tau\tau} u_1 + \Gamma |u_1|^2 u_1 = 0, \quad (1)$$

whereas SH generation is ruled by the vector NLS model

$$\begin{aligned} (i\partial_\zeta + \sigma_1 \nabla_\perp^2 - d_1 \partial_{\tau\tau}) u_1 + \Gamma u_2 u_1^* e^{i\delta k \zeta} &= 0, \\ (i\partial_\zeta + \sigma_2 \nabla_\perp^2 + iv \partial_\tau - d_2 \partial_{\tau\tau}) u_2 + \Gamma \frac{u_1^2}{2} e^{-i\delta k \zeta} &= 0. \end{aligned} \quad (2)$$

In Eqs. (1) and (2) the link with real-world variables X, Y, Z, T is as follows: $\zeta \equiv Z/Z_{\text{df}}$ is the propagation distance in units of diffraction length $Z_{\text{df}} = 2k_1 W_0^2$ associated with the beam waist W_0 , $\nabla_\perp^2 \equiv \partial_\xi^2 + \partial_\eta^2$ is the transverse Laplacian, $(X, Y) = W_0(\xi, \eta)$, and $\tau = (T - k'_1 Z)/T_0$ is the retarded time [in units of $T_0 = (|k'_1| Z_{\text{df}}/2)^{1/2}$] in a frame moving with group velocity $1/k'_1$ of u_1 , k''_m ($m = 1, 2$) being GVDs at $m\omega_0$. The coefficients are $d_m = k''_m/|k'_1|$, $\sigma_m = k_1/k_m$ ($\sigma_2 \simeq 1/2$), the wave-number mismatch $\delta k = (k_2 - 2k_1)Z_{\text{df}}$, and $\Gamma = Z_{\text{df}}/Z_{\text{nl}}$ quantifies the impact of nonlinearities. Here $Z_{\text{nl}} = (\chi_3 I_p)^{-1}$ in Eq. (1) and $Z_{\text{nl}} = (\chi_2 \sqrt{I_p})^{-1}$ in Eqs. (2) (χ_3 [m/W] and χ_2 [W^{-1/2}] are standard nonlinear coefficients) are nonlinear lengths associated with input peak intensity I_p at ω_0 . The complete real-world fields are $E_m(X, Y, Z, T) = (I_p/m)^{1/2} u_m(\xi, \eta, \zeta, \tau) \exp(ik_m Z - im\omega_0 T)$, $m = 1, 2$. Finally, $v = Z_{\text{df}}(k'_2 - k'_1)/T_0$ measures the impact of group-velocity mismatch (GVM), though we deal mainly with Eqs. (2) in the velocity matched case $v = 0$.

We seek for luminal (the barycenter moves with velocity $1/k'_1$), propagation-invariant, radially symmetric LWP of the form $u_1 = f_1(r, t) \exp(-i\beta\zeta)$, accompanied in Eqs. (2) by a symbiotic SH $u_2 = f_2(r, t) \exp[-i(2\beta + \delta k)\zeta]$. Here f_m ($m = 1, 2$) is real and $m\beta$ stands for the normalized nonlinear deviation from the linear wave number k_m , which can eventually vanish ($\beta = 0$). In the cubic case, f_1 obeys the equation

$$\dot{f}_1 + r^{-1}\dot{f}_1 - D_1\partial_{tt}f_1 + bf_1 + \gamma f_1^3 = 0, \quad (3)$$

while Eqs. (2) yield (after setting $f_1/\sqrt{\sigma_2} \rightarrow f_1$)

$$\begin{aligned} \ddot{f}_1 + r^{-1}\dot{f}_1 - D_1\partial_{tt}f_1 + bf_1 + \gamma f_2 f_1 &= 0, \\ \ddot{f}_2 + r^{-1}\dot{f}_2 - D_2\partial_{tt}f_2 + \alpha f_2 + \gamma \frac{f_1^2}{2} &= 0, \end{aligned} \quad (4)$$

where we have set $D_m = d_m/\sigma_m$, $\dot{f} = \partial f/\partial r$, and $r = |\beta|^{1/2}\rho$ ($r^2 \equiv x^2 + y^2$, $\rho^2 \equiv \xi^2 + \eta^2$), $t = |\beta|^{1/2}\tau$, $\gamma = \Gamma/|\beta|$, $b = \beta/|\beta|$, and $\alpha = (2b + \delta k/|\beta|)/\sigma_2$ in the nondegenerate case ($\beta \neq 0$), while $(r, t) = (\rho, \tau)$, $\alpha = \delta k/\sigma_2$, $\gamma = \Gamma$, and $b = 0$ in the degenerate case ($\beta = 0$). The ζ -independent Eqs. (3) and (4) must be integrated along with the boundary conditions $f_{1,2}(r, t, \pm\infty) = f_{1,2}(\infty, t) = 0$, and $\dot{f}_{1,2}(0, t) = 0$. While the anomalous GVD regime ($D_m < 0$) guarantees that, for $\beta < 0$ ($b, \alpha < 0$), nearly separable LWP (light bullets) exist with exponentially decaying tails [9], in the normal GVD regime ($D_m > 0$) the nature of the LWP solutions (if any) must change dramatically, because the low-intensity exponential damping no longer takes place. Pseudospectral numerical techniques, i.e., reducing Eqs. (3) and (4) to a dynamical set of ordinary differential equations in r by means of appropriate discretization in t [16], are well suited to search for strongly nonseparable objects with slow spatiotemporal decay. We have implemented such methods and found LWP when $\beta \geq 0$ ($b, \alpha \geq 0$). Efficient convergence occurs by employing as a trial function (of time, at $r = 0$) the real part of the waveform,

$$u_m = \frac{1}{\sqrt{[\Delta - i(\tau/d_m)]^2 + \rho^2}}; \quad m = 1, 2, \quad (5)$$

which represent X-shaped LWP solutions of Eqs. (1) and (2) in the *linear limit* ($\Gamma = 0$). Here Δ is a free parameter: the smaller Δ , the stronger the localization. The LWP solutions, obtained from Eq. (3) with $\Delta = 1$ in Eq. (5) are shown in Fig. 1. For $b = 0$ and moderate nonlinearities [$\gamma = 1$, Fig. 1(a)], the ‘‘ground-state’’ LWP mode has a clear X shape (in $x - t$ at $y = 0$), or V shape in $r - t$ plane, encompassing a space-time tightly confined structure, with slow ($1/r$) axisymmetric spatial decay accompanied by temporal pulse splitting occurring only off axis. In the case $b = 1$, while the field maintains its basic X shape, it develops radial (damped) oscillations as shown in Fig. 1(b), e.g., for the strong nonlinear case ($\gamma = 10$).

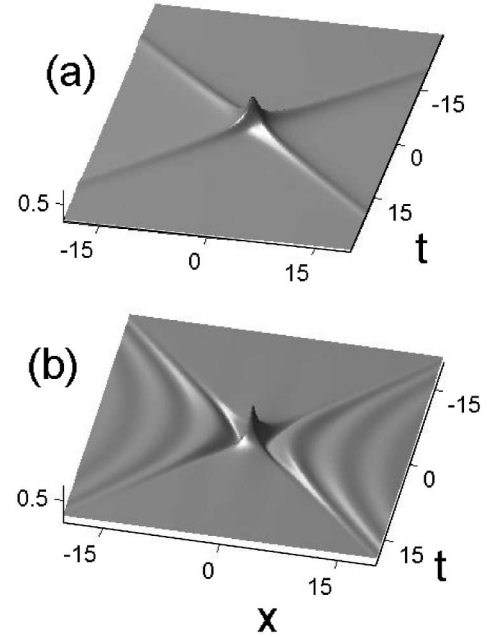


FIG. 1. NLXWs in Kerr media as obtained from Eq. (3) with (a) $b = 0$, $\gamma = 1$; (b) $b = 1$, $\gamma = 10$. We display the propagation invariant profile $f_1(r, t)$ as seen on the plane $y = 0$, i.e., $f_1(x, y = 0, t)$. Revolution around the $x = 0$ axis yields the full biconical structure of NLXWs in (x, y, t) space.

From Eqs. (4) we obtain similar NLXWs, where the two symbiotic LWP f_1 - f_2 can be both of ground-state type ($b = \alpha = 0$), ground-oscillatory type ($b = 0$, $\alpha \neq 0$), or both of oscillatory type ($b = 1$, $\alpha \neq 0$), an example of the latter case being shown in Fig. 2.

In both nonlinear processes the oscillations stem from the fact that the spatial behavior of the low-intensity portion of the LWP is governed by a zeroth order Bessel equation, which can be easily obtained by Fourier transforming the linear ($\gamma = 0$) limit of Eq. (3) or (decoupled) Eqs. (4). Therefore NLXWs exhibit the characteristic damped spatial oscillations of J_0 Bessel functions, and can be regarded as the natural generalization of monochromatic nondiffractive conical J_0 beams, whose physical realization was demonstrated both in the linear [13] and nonlinear [17] regimes.

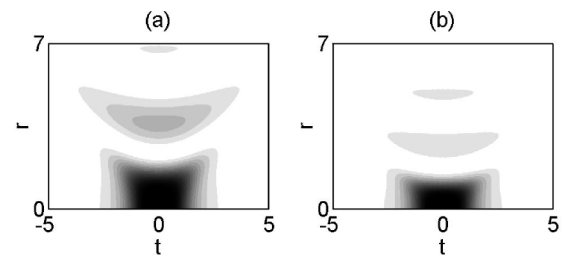


FIG. 2. NLXW spatiotemporal intensity (a) $|u_1(t, r)|^2$; (b) $|u_2(t, r)|^2$, obtained from Eqs. (4) with $b = 1$, $\alpha = 2$, $\gamma = 1$. Note the out-of-phase oscillations between the two fields.

More precisely, once the NLXW solutions $f_m = f_m(r, t)$ are obtained, they can be represented in the spectral domain of transverse wave vector $K = (K_x^2 + K_y^2)^{1/2}$ and frequency detuning Ω , through the Fourier-Bessel transform $S_m = S_m(K, \Omega)$, as

$$f_m = \int_0^{+\infty} \int_{-\infty}^{+\infty} S_m(\Omega, K) J_0(Kr) e^{i\Omega t} K dK d\Omega, \quad (6)$$

showing their nature of a weighted superposition of conical J_0 beams with different frequency.

Compared with their anomalous GVD counterparts [i.e., (1 + 3)D bullet LWPs], NLXWs exhibit important differences: (i) NLXWs experience weaker localization ($1/r$ instead of exponential decay). As a consequence, the energy of our NLXW solutions is infinite [e.g., in Eq. (1), $\mathcal{E}_1 = \int_0^a r dr \int_{-\infty}^{\infty} dt |u_1|^2$ diverges as the computational window $a \rightarrow \infty$]. This is not surprising since also energy of linear X waves (5) or power of J_0 beams [13] are infinite. In analogy with the linear regime where finite-energy X waves exist [14,15,18], we expect that finite-energy NLXWs can be generated in real-world experiments. (ii) Unlike bullets that vanish in the linear limit, NLXWs have a finite limit for $\Gamma = 0$. (iii) NLXWs are not unique, in the sense that infinitely many solutions can be found for fixed β and Γ . This follows also from (ii) since linear paraxial X waves are a continuous family, e.g., parametrized by Δ in Eq. (5). (iv) NLXWs and bullets exist for different signs of β , entailing opposite phase shifts in Kerr media, and different constraints ($\beta \leq -\delta k/2$ for NLXWs, $\beta < \delta k/2$ for bullets) in Eqs. (2).

Once the existence of nonlinear LWPs supported by normal GVD is established, one might wonder about their importance and observability. In the linear regime, both Durnin J_0 beams [13] and nonmonochromatic X-shaped LWPs [15] can be observed only by means of experimental arrangements that adapt the input to the LWP (e.g., by means of lensacons or axicons). Vice versa, we have found that the interplay of the nonlinearity and normal GVD is responsible for a universal mechanism, namely, colored conical emission (CE), that allows for the self-induced spectral (in Ω - K) reshaping necessary to turn conventional, e.g., Gaussian, pulsed beams into X waves. In fact, both in Kerr media [19] and SH generation [20], the (modulational) stability analysis of cw plane-wave solutions yields exponential amplification of conical plane-wave (or Bessel J_0) perturbations with transverse wave vector K and frequency detuning Ω . In the normal GVD regime ($d_m > 0$), the form of the instability gain entails CE, i.e., preferential amplification of waves at K (angles) linearly increasing with frequency detuning Ω . By comparing (see Fig. 3) the CE gain with the NLXW spectrum, obtained by inverting Eq. (6), it is clear that the instability provides amplification at $K - \Omega$ pairs that favors the formation of NLXWs. Although the stability analysis is carried out for cw plane-wave pumping beams, CE

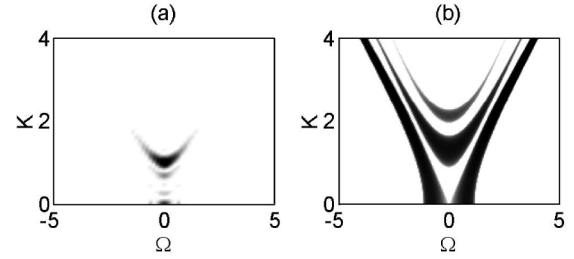


FIG. 3. Comparison of NLXW and CE gain in the spectral domain: (a) $|S_1(K, \Omega)|$ transform of the field u_1 in Fig. 2(a) ($|S_2(K, \Omega)|$ is similar); (b) CE domains for the out-of-phase cw plane-wave eigenmode with the same parameters.

occurs also from tightly focused short-pulse input beams [19]. In this case, we expect CE to amplify frequencies $K - \Omega$ contained in the broad input spectrum, while preserving the phase coherence between different spectral components characteristic of NLXWs.

In order to support this conjecture and show that NLXWs can be generated in experiments we have integrated numerically the propagation models Eqs. (1) and (2) with input (at $Z = 0$) wave packets of the standard Gaussian type (in X, Y, T). Since their input energy is finite, this permits one to also establish whether finite-energy NLXWs can be observed. As far as the Kerr case is concerned, our simulations show clear evidence of NLXW formation for the appropriate choice of duration and width at peak power below twice the self-focusing critical power [3] (details will be reported elsewhere). However, such a mechanism competes with conventional pulse-splitting (temporal splitting also on axis without the localized peak characteristic of a NLXW), which is found to prevail in a wide range of input conditions, in agreement with previous simulations [3,4,10]. Clear indications for experiments are further complicated by the impact that higher-order effects not included in Eq. (1) (Raman, self-steepening, space-time coupling, saturation, etc.) are known to have [4,10]. Conversely, we find that stable excitation of NLXW occurs in SH generation in the large negative mismatch limit, where the field u_1 plays a leading role and experiences an effective Kerr-type self-focusing, described with reasonable accuracy by Eqs. (2) also in the subpicosecond regime [1,6]. Specifically, we refer to the case of lithium triborate (LBO), for which preliminary experimental data indicate the occurrence of pulse compression (in spite of normal GVD) and NLXW formation [21]. We model the latter case assuming $\chi_2 \approx 7 \times 10^{-5} \text{ W}^{-1/2}$, $k_1'' = 0.016 \text{ ps}^2/\text{m}$, $k_2'' = 0.089 \text{ ps}^2/\text{m}$, a mismatch $\Delta k = -30 \text{ cm}^{-1}$ ($\delta k = -180$), and a spatio-temporal input Gaussian beam $u_1(Z = 0)$ with FWHM 170 fsec duration and $65 \mu\text{m}$ beam width. Figures 4(a) and 4(c) show the output intensity after $L = 4 \text{ cm}$ propagation in the ideal GVM-matched case for an input intensity $I_p = 50 \text{ GW}/\text{cm}^2$ ($Z_{nl} = 0.6 \text{ mm}$). As shown, while a moderate fraction of the energy lags behind and

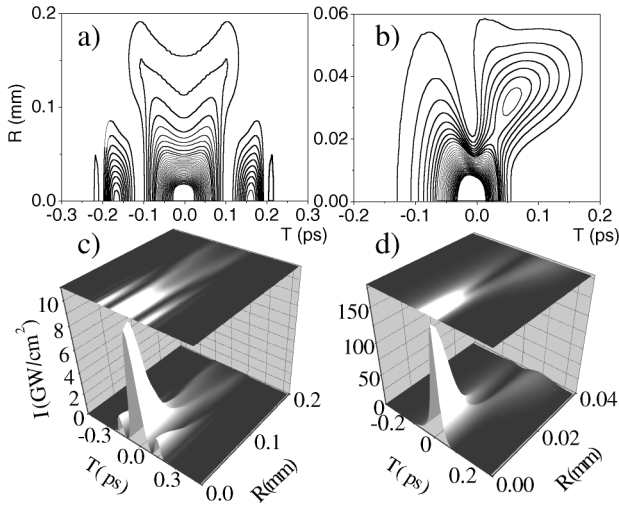


FIG. 4. Contour lines (a),(b) in time-radial plane $T, R = \sqrt{X^2 + Y^2}$, and corresponding 3D plots (c),(d) of real-world output intensity $|E_1(R, T, Z = L)|^2$ obtained from integration of Eqs. (2). (a)–(c) shows the velocity matched case $v = 0$, whereas (b)–(d) are relative to nonzero GVM ($v \neq 0$). See text for coefficient values.

in front in the form of pulse satellites, the main portion of the beam develops the characteristic structure of a NLXW. Importantly, we observe that the formation of a NLXW type of LWP in Fig. 4 is accompanied by strong pulse compression. In fact, the peculiar spatiotemporal structure of a NLXW leads to an effective GVD $k''_{\text{eff}} \equiv \frac{d^2 k_z}{d\omega^2} \simeq \frac{d^2}{d\omega^2} [k(\omega) - \frac{k_t^2}{2k_0}] \simeq k'' - k_1 (\frac{d\theta}{d\omega})^2$, where the angle $\theta \simeq \sin\theta = k_t/k_1$, and $k_t = (k_1^2 - k_z^2)^{1/2} = |\beta|^{1/2} K/W_0$. Therefore the dispersive contribution which stems from the angular dispersion $\theta = \theta(\omega)$ counteracts the material (normal) GVD, leading to an effective anomalous GVD, which in turn explains the compression.

NLXWs are robust also against strong GVM. First, when $v \neq 0$ in Eqs. (2), we find CE as well as NLXW solutions of Eqs. (2) characterized by an additional complex phase profile. On the other hand, our simulations show that, at sufficiently high intensity, after a short distance, the launched (u_1) and generated (u_2) fields tend to develop spontaneously NLXW shapes, meanwhile leading to nonlinear walk-off compensation ($u_{1,2}$ travel locked together). For instance, in Figs. 4(b) and 4(d) we show the intensity profile obtained for an input intensity $I_p = 70 \text{ GW/cm}^2$ after $L = 1.5 \text{ mm}$ propagation in LBO at $\lambda = 1.06 \mu\text{m}$, where a GVM as large as $\delta V = 45 \text{ ps/m}$ ($v = 75$) is compensated.

Our results show that, contrary to common belief, nonlinear space-time localization takes place also in normally dispersive media. NLXWs can be envisaged to be eigenmodes of several (1 + 3)D paraxial wave propagation models, and open new perspectives in the interpretation of space-time coupling. Further work will be necessary to search for NLXW solutions with finite en-

ergy (of which we have given numerical evidence), and/or subluminal or superluminal nature, as well as the role played by nonparaxiality and higher-order nonlinear terms.

Funds from MIUR (PRIN01 and FIRB projects) and Unesco UVO-ROSTE (Contract No. 875.586.2) are gratefully acknowledged. J.T. thanks Secretaria de Estado y Universidades, Spain. C. C. thanks Fondazione Tronchetti Provera.

*Also at Department Fisica i Enginyeria Nuclear, UPC Terrassa, Spain.

- [1] *Spatial Solitons*, edited by S. Trillo and W. E. Torruellas (Springer, Berlin, 2001).
- [2] G. P. Agrawal, *Nonlinear Fiber Optics* (Academic Press, New York, 1995).
- [3] J. K. Ranka, R. W. Schirmer, and A. L. Gaeta, *Phys. Rev. Lett.* **77**, 3783 (1996).
- [4] A. A. Zozulya, S. A. Diddams, A. G. Van Engen, and T. S. Clement, *Phys. Rev. Lett.* **82**, 1430 (1999).
- [5] H. S. Eisenberg *et al.*, *Phys. Rev. Lett.* **87**, 043902 (2001).
- [6] X. Liu, L. J. Qian, and F. W. Wise, *Phys. Rev. Lett.* **82**, 4631 (1999).
- [7] I. G. Koprnikov *et al.*, *Phys. Rev. Lett.* **84**, 3847 (2000); A. L. Gaeta and F. Wise, *Phys. Rev. Lett.* **87**, 229401 (2001).
- [8] S. Tzortzakakis *et al.*, *Phys. Rev. Lett.* **87**, 213902 (2001).
- [9] J. I. Gersten and N. Tzoar, *Phys. Rev. Lett.* **35**, 934 (1975); Y. Silberberg, *Opt. Lett.* **15**, 1282 (1990).
- [10] B. Gross and J. T. Manassah, *Opt. Commun.* **129**, 143 (1996); **158**, 105 (1998); M. Trippenbach and Y. B. Band, *Phys. Rev. A* **56**, 4242 (1997).
- [11] P. R. Stepanishen and J. Sun, *J. Acoust. Soc. Am.* **102**, 3308 (1997); J. Salo, J. Fagerholm, A. T. Friberg, and M. M. Salomaa, *Phys. Rev. Lett.* **83**, 1171 (1999).
- [12] J. Salo, J. Fagerholm, A. T. Friberg, and M. M. Salomaa, *Phys. Rev. E* **62**, 4261 (2000); K. Reivelt and P. Saari, *J. Opt. Soc. Am. A* **17**, 1785 (2000).
- [13] J. Durnin, J. J. Miceli, and J. H. Eberly, *Phys. Rev. Lett.* **58**, 1499 (1987).
- [14] J. Lu and J. F. Greenleaf, *IEEE Trans. Ultrason. Ferroelectr. Freq. Control* **39**, 441 (1992).
- [15] P. Saari and K. Reivelt, *Phys. Rev. Lett.* **79**, 4135 (1997); H. Sönajalg, M. Rätsep, and P. Saari, *Opt. Lett.* **22**, 310 (1997).
- [16] C. Canuto *et al.*, *Spectral Methods in Fluidodynamics* (Springer, New York, 1988).
- [17] P. Di Trapani *et al.*, *Phys. Rev. Lett.* **81**, 5133 (1998).
- [18] M. Zamboni-Rached, E. Recami, and H. E. Hernandez-Figueroa, *physics/0109062*.
- [19] L. W. Liou, X. D. Cao, C. J. McKinstrie, and G. P. Agrawal, *Phys. Rev. A* **46**, 4202 (1992); G. G. Luther, A. C. Newell, J. V. Moloney, and E. M. Wright, *Opt. Lett.* **19**, 789 (1994).
- [20] S. Trillo *et al.*, *Opt. Lett.* **27**, 1451 (2002).
- [21] P. Di Trapani *et al.*, *physics/0303083*.